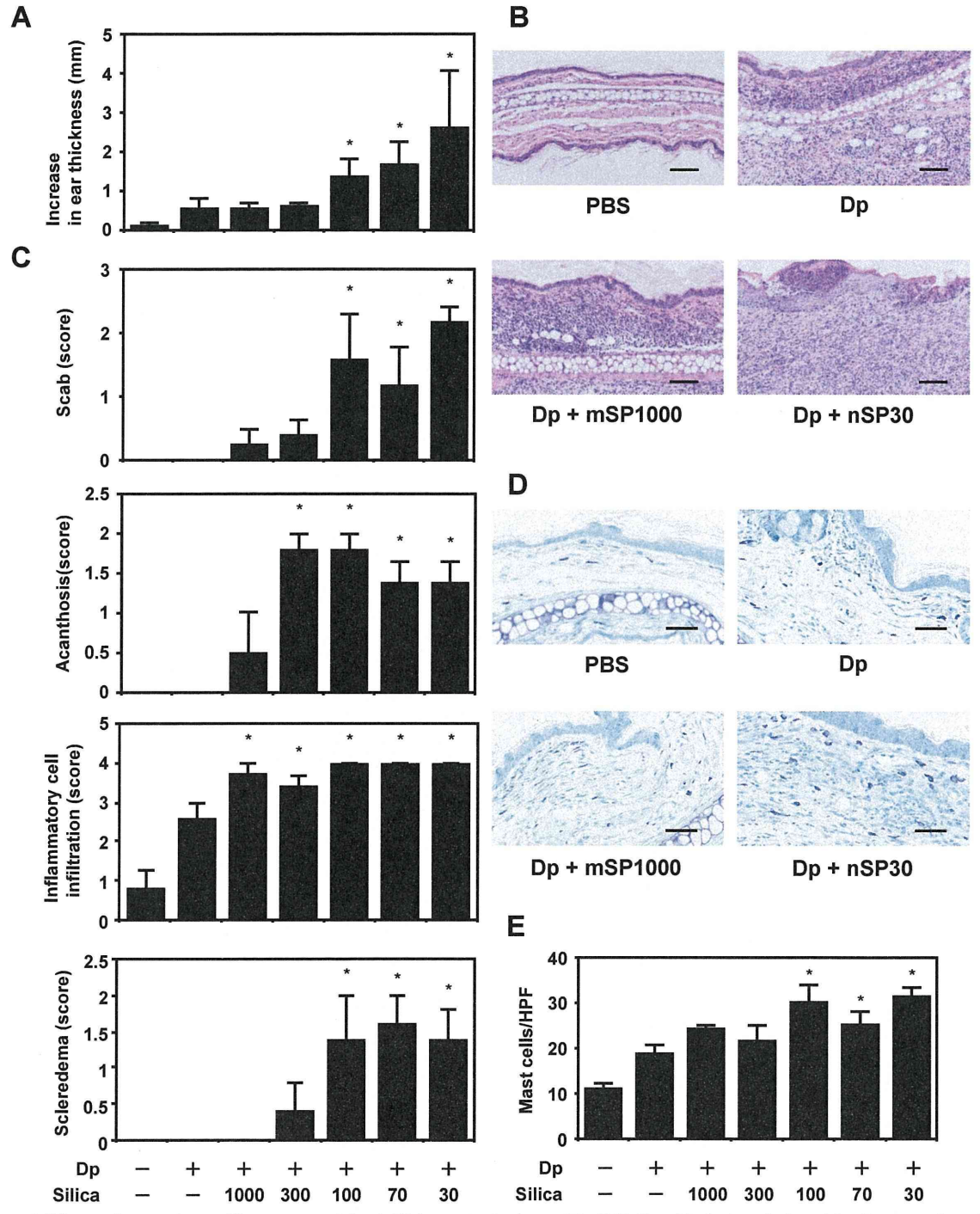

Figure 1 Effects of amorphous silica nanoparticles (nSPs) on atopic dermatitis (AD)-like skin lesions induced by *Dermatophagoides pteronyssinus* (Dp). NC/Nga mice were intradermally injected on the ventral side of both ears with Dp alone or Dp plus SPs in PBS on days 1, 3, 5, 7, 9, 11, 13, 16, and 18. Ear thickness was measured on days 0 and 19 (A). The ears were removed 24 h after the last intradermal injection. Sections were prepared, and the ears were stained with H&E to assess representative symptoms of AD (B and C) or with toluidine blue to assess mast cell infiltration (D and E). Representative histological findings of the PBS, Dp, Dp + mSP1000, and Dp + nSP30 groups are shown. Several representative symptoms of AD were scored in the H&E sections (C). Infiltration of mast cells was evaluated as the number of cells in toluidine blue sections in a high power field (E). Data are presented as mean ± SE of 4-5 animals per group. The results are representative of two separate experiments. *P < 0.05 vs. Dp group. Scale bars: 100 μm (B) and 50 μm (D).

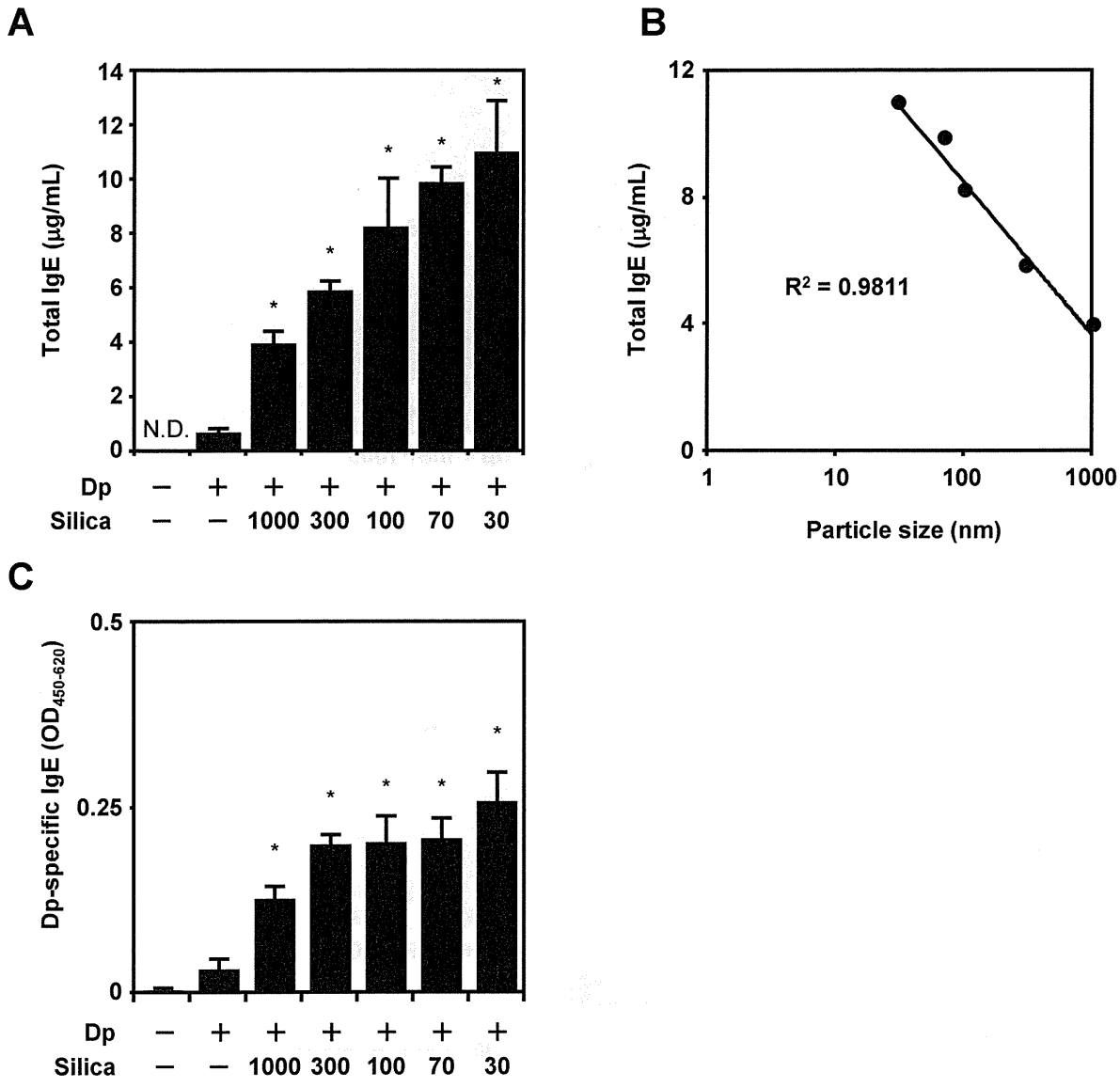

Figure 2 Effects of amorphous silica particles (SPs) on total and *Dermatophagoides pteronyssinus* (Dp)-specific IgE production in plasma. NC/Nga mice were intradermally injected on the ventral side of both ears with Dp alone or Dp plus SPs in PBS on days 1, 3, 5, 7, 9, 11, 13, 16, and 18. To evaluate AD severity, plasma was collected 24 h after the last intradermal injection and analyzed by ELISA for total and Dp-specific IgE (A and C). A regression analysis of total IgE was also performed (B). Data are presented as mean ± SE of 4-5 animals per group. The results are representative of two separate experiments. *P < 0.05 vs. Dp group.

were not paralleled with the size of SPs. Thus, nSP-mediated aggravation of AD-like lesions has more to do with total IgE than Dp-specific IgE.

Cytokine expression analysis of nSP-injected skins

To clarify the mechanism of AD-like skin lesions enhanced by SPs, we analyzed the cytokine expression profile in the skin related to Dp. We examined the levels of Th2-type cytokines (IL-4, IL-5, and IL-13), Th1-type cytokines IFN-γ, IL-18, and thymic stromal lymphopoietin (TSLP) in the ears 24 h after the last intradermal injection (Figure 3). Intradermal injection of Dp alone increased the local expression of IL-4 and IL-13 and decreased the production of IL-5 and IFN-γ compared with PBS injection. Only differences of the expression of IL-13 between the Dp group and PBS group is significant. In contrast, the level of IL-4 in the Dp + SP groups with diameters ≤300 nm increased significantly

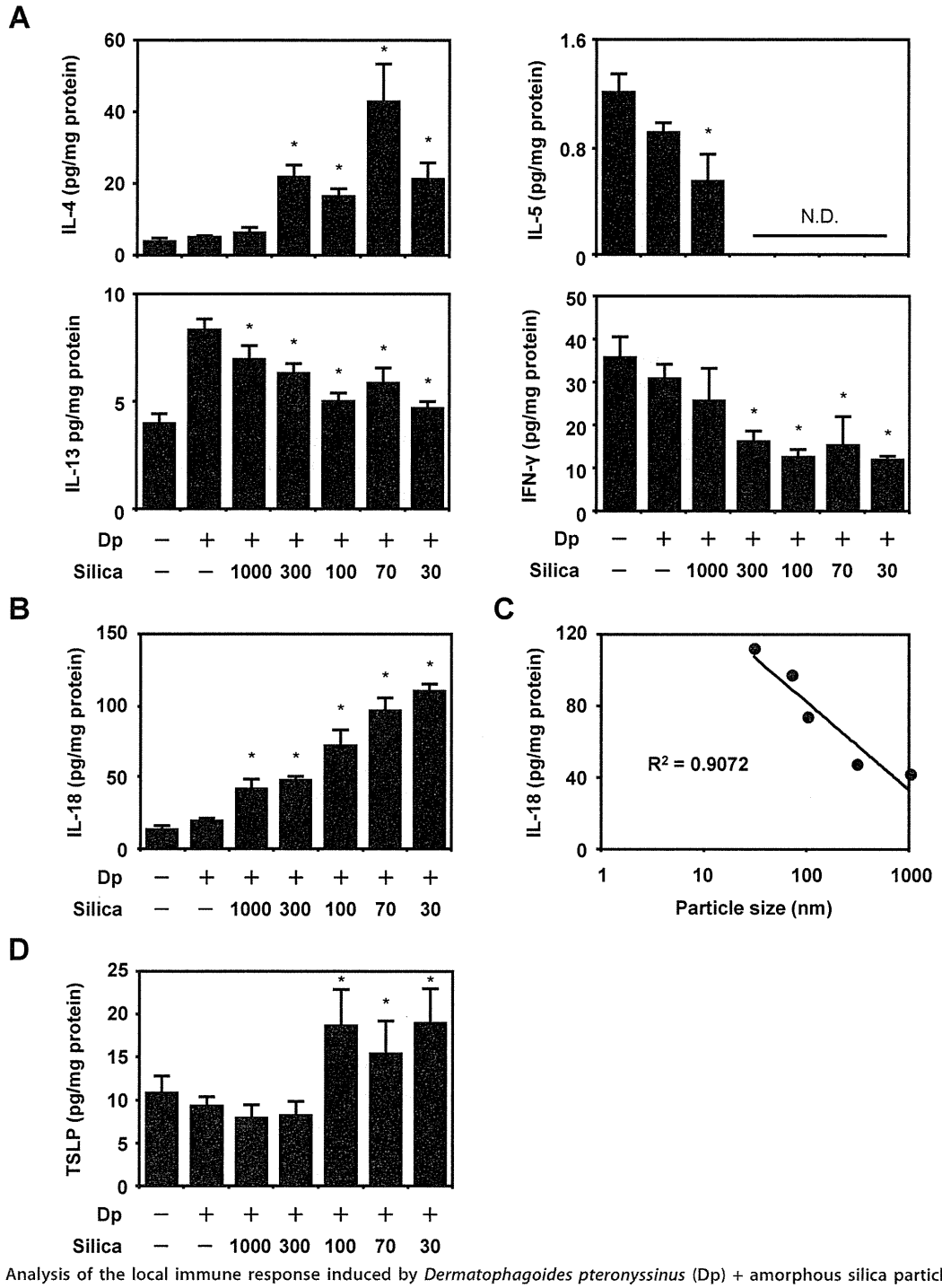

Figure 3 Analysis of the local immune response induced by *Dermatophagoides pteronyssinus* (Dp) + amorphous silica particles (SPs). NC/Nga mice were intradermally injected on the ventral side of both ears with Dp alone or Dp plus SPs in PBS on days 1, 3, 5, 7, 9, 11, 13, 16, and 18. At 24 h after the last intradermal injection, the ears were removed and homogenized. The homogenates were centrifuged at 10,000 rpm for 5 min, and the supernatants were collected. The levels of interleukin (IL)-4, IL-5, IL-13, interferon (IFN)-γ, IL-18, and thymic stromal lymphopoietin (TSLP) in the supernatants were examined by ELISA (A, B, and D). A regression analysis of IL-18 was also performed (C). Data are presented as mean ± SE of 4-5 animals per group. The results are representative of two separate experiments. *$P < 0.05$ vs. Dp group.

compared with that in the Dp alone group. The levels of IL-5 and IL-13 in the Dp + SP groups with a diameter ≤300 nm decreased significantly compared with those in the Dp alone group. Additionally, injections of SPs with a diameter ≤300 nm led to a significant decrease in IFN-γ compared to those of Dp alone (Figure 3A). Thus, the injection of SPs with Dp tended to enhance the effects of injecting Dp alone in terms of cytokine levels in the skins. However, the levels of IFN-gammma and IL-5 were significantly reduced after SPs treatment when compared to Dp only. The levels of IL-18, known as an AD-inducing cytokine, were higher in the Dp + smaller SP groups than those in the Dp alone group (Figure 3B). A regression analysis showed that the particle size reduction was a significant contributor to this effect (Figure 3C; R^2 = 0.91). IL-18 production size-dependently increased similar to that of plasma total IgE levels. Furthermore, the levels of TSLP, an AD-inducing cytokine, were enhanced in only the Dp + nSP groups compared with those in the Dp alone group (Figure 3D). This result matched that of increase in ear thickness.

Dp-specific immune response in Dp + SPs-injected mice

To evaluate the effect of SPs on systemic immune responses, we examined the levels of Dp-specific IgG and its subtypes by ELISA 24 h after the last intradermal injection (Figure 4A and 4B). Higher levels of Dp-specific IgG were observed in the Dp + SP groups than those in the Dp alone group (Figure 4A). Furthermore, higher Dp-specific IgG levels were observed, particularly in Dp + nSP groups. Dp-specific IgG1 levels in the Dp + SP groups were higher than those in the Dp alone groups. In contrast, the levels of Dp-specific IgG2a were low in all groups except the Dp + nSP30 group. Plasma IgG subclass responses have been used to assess the type of immune response. It is well-known that IgG1 is indicative of a Th2-type response, whereas IgG2a is indicative of a Th1 response. Therefore, these results indicate that Dp + SPs induced antigen-specific Th2-type immune responses and that Dp + nSP30 induced not only Th2-type immune responses but also Th1-type responses.

To further characterize the type of systemic immune response, we measured the levels of Dp-specific IFN-γ- and IL-4-secreting splenocytes from each intradermally injected mouse using a cytokine-specific ELISPOT assay (Figure 4B). The number of Dp-specific IFN-γ-secreting splenocytes in the Dp + nSP30 group was significantly greater than that in all other groups. However, no difference was observed in the Dp-specific IFN-γ-secreting splenocytes of all groups except the Dp + nSP30 group. These levels of Dp-specific IFN-γ-secreting splenocytes were correlated with Dp-specific IgG2a levels. The levels of Dp-specific IL-4-secreting splenocytes in the Dp + SP groups were enhanced in a SP size-dependent manner compared with those in the Dp alone group (Figure 4C). The regression analysis showed that the particle size reduction was a significant contributor to this effect (Figure 4D; R^2 = 0.93). Thus, the levels of Dp-specific IL-4-secreting splenocytes paralleled AD severity.

Discussion

The lifetime prevalence of AD is estimated at 15-30% in children and 2-10% in adults, and the incidence of AD has increased by two- to threefold during the past three decades in industrialized countries [16,17]. Although environmental factors and lifestyle changes are speculated to be associated with the increased number of patients with AD, the detailed relationships between environmental factors or lifestyle changes and the increase in AD are not well understood. Some epidemiological studies have shown that chronic exposure to urban fine particles could be a risk factor for AD [18,19]. In addition, $nTiO_2$ and polystyrene nanoparticles have been reported to exacerbate AD [20,21]. Thus, among other environmental factors, NMs may be a risk factor for the onset or aggravation of AD. However, the relationship between AD and nSPs, which are one of the most widely used NMs in various applications, has never been investigated. Here, to clarify the relationship between NM use and the onset or aggravation of AD, we investigated the effects of nSPs on AD-like skin lesions induced by a mite allergen Dp.

Typical symptoms of AD, such as inflammation or itching of the skin, are induced by chemical mediators such as histamine and some cytokines [22,23]. Furthermore, these chemical mediators or cytokines are induced by IgE or antigen cross-linking of IgE bound to FcεRI on mast cells [24]. We measured Dp-specific IgE to determine allergen-specific IgE participation in the aggravation of AD. As expected, the Dp-specific IgE level was higher in the Dp + SP groups than that in the Dp alone group (Figure 2C). Because particle materials influence the intracellular processing of antigen in antigen-presenting cells (APCs) such as dendritic cells (DCs) [25,26], it is possible that SPs affected these APCs and changed the Dp-specific immune responses. However, these Dp-specific IgE levels were not dependent on SP size and were not high in the Dp + nSP groups compared with those in the Dp + submicron-sized SPs groups. In contrast, a regression analysis showed that the total IgE levels, which are known to correlate with AD severity [27,28], were completely dependent on injected SP size (Figure 2A; R^2 = 0.98). Thus, this result suggested that smaller SPs induced more severe AD and, most importantly, that the mechanisms of AD aggravation caused by SPs were induced not only by

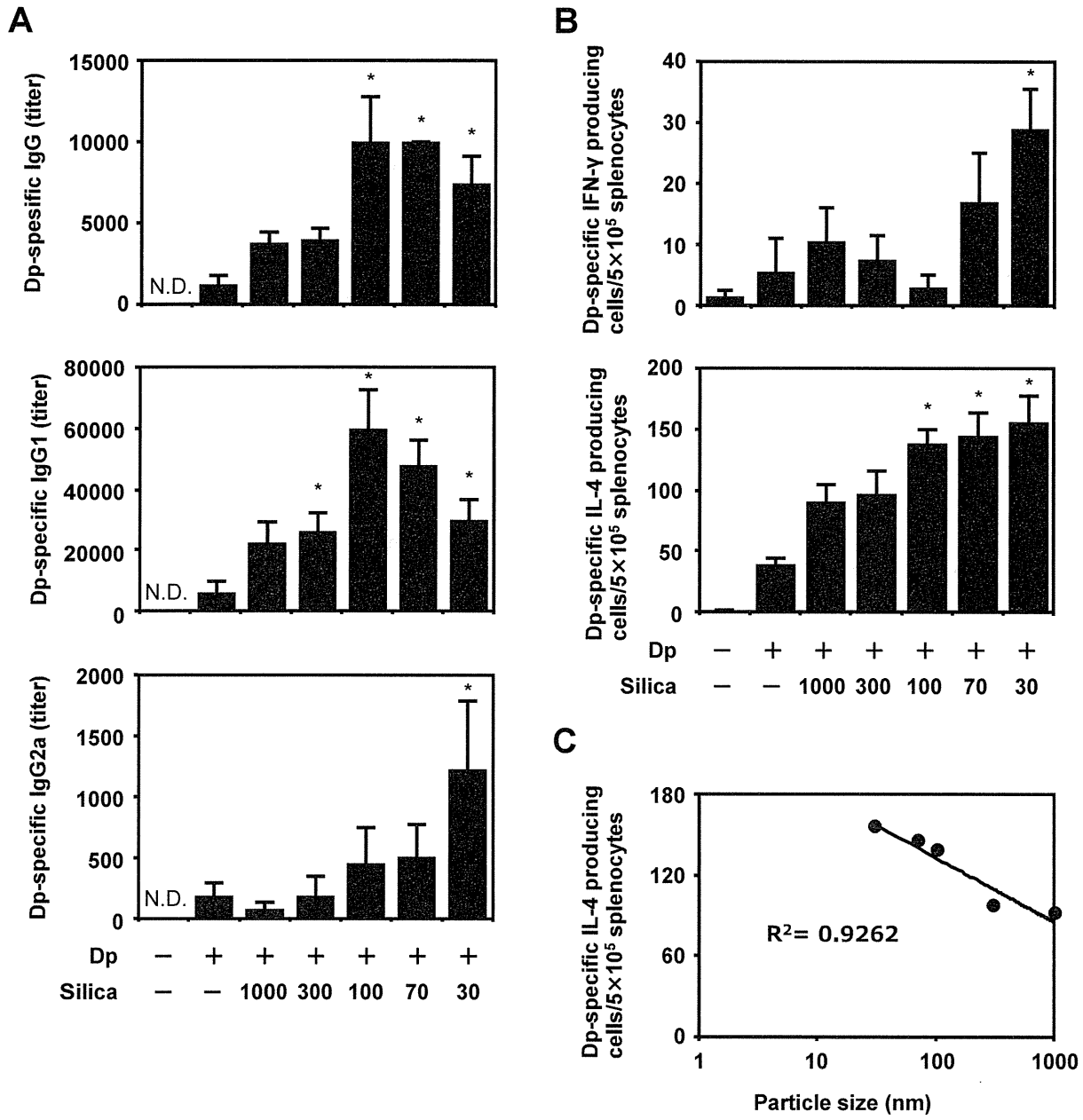

Figure 4 Analysis of the systematic immune response induced by *Dermatophagoides pteronyssinus* (Dp) + amorphous silica particles (SPs). NC/Nga mice were intradermally injected on the ventral side of both ears with Dp alone or Dp plus SPs in PBS on days 1, 3, 5, 7, 9, 11, 13, 16, and 18. At 24 h after the last intradermal injection, splenocytes and plasma were collected from each group. Dp-specific IgG and its subclasses (A) in plasma were analyzed by ELISA. Splenocytes from each group were cultured with 100 μg ml^{-1} Dp. The levels of Dp-specific interferon (IFN)- γ and interleukin (IL)-4-producing cells were examined by individual cytokine-specific ELISPOT assay (B). A regression analysis of Dp-specific IL-4-producing cells was also performed (C). Data are presented as mean ± SE of 4-5 animals per group. The results are representative of two separate experiments. *P < 0.05 vs. Dp group.

Dp-specific IgE. Thus, the mechanisms different from the mechanisms correlated with Dp-specific IgE production were also involved in this model. Therefore, clarification of the mechanisms of size-dependent aggravation of AD-like skin lesions is important for a risk analysis of nSPs and for designing safer forms of nSPs.

AD skin lesions are characterized by recruitment of lymphocytes, monocytes, eosinophils, and mast cells

[29,30]. These infiltrating cells produce Th2 cytokines including IL-4 and IL-13. These mediators promote Th2 deviation not only in acute eczematous skin lesions but also in systemic adaptive immune systems [31,32]. This Th2 deviation could further compromise barrier function in the skin lesions and complete a potential outside-inside-outside pathogenic loop of AD [33]. Additionally, IL-18 or TSLP plays a critical role in the spontaneous development of AD [34,35]. Considering this, we first performed an analysis of the Th1/Th2 cytokine balance in the skin lesions to clarify the mechanism of AD aggravation by SPs. Although IL-4 levels in the ears increased, IL-5, IL-13, and IFN-γ levels decreased following exposure to Dp + SPs compared with those following exposure to Dp alone (Figure 3). There is possible that variously sized SPs induced the expression of Th2 cytokines at an early phase and that this induction might contribute to the aggravation of symptoms. A time-course study is needed to elucidate the correlation between symptoms and inflammatory mediators.

Epithelial cells are major cell source of various pro-allergic cytokines, such as IL-18 and TSLP. As they are accumulated preferentially in the inflammatory sites of patients with AD, IL-18 and TSLP might be involved in the development of AD [16,36]. To reveal the mechnisms of the nSPs-mediated aggravation of AD-like skin lesion, we performed further analyses to measure IL-18 and TSLP levels in the skin. Interestingly, the IL-18 levels in skin lesions of the Dp + SP groups increased compared to those in the Dp alone group in a SP size-dependent manner (Figure 3; $R^2 = 0.91$). IL-18 is a cytokine that stimulates mast cells and basophils to release AD-associated molecules, Th2 cytokines, and histamine, without a pathway that involves Ag, IgE, or FcRI. Furthermore, IL-18 induces large amounts of total IgE via natural killer T and $CD4^+$ T cells [37-39]. These effects of IL-18 finally induce AD-like skin lesions [34]. Considering these, this IL-18 production in a size-dependent manner of SPs show why smaller SPs induced severe AD accompany the production of total IgE. On the other hands, the TSLP levels were only increased following the exposure to Dp + "nSPs" (Figure 3). This result is similar to those of increase in ear thickness, scab and scleredema. TSLP can promote the Th2 cytokine-associated inflammation by directly promoting the effector functions of $CD4^+$ Th2 cells, basophils and other granulocyte populations via DC [35,40]. Furthermore, it is reported that skin-specific overexpression of TSLP resulted in an AD-like skin lesion [35,40]. Thus, these results suggested that TSLP as well as IL-18 might be involved in the development of nSP-mediated AD-like skin lesions in mice. Although we need further mechanistic studies for understanding the nSP-mediated production of IL-18 and TSLP, modification of physicochemical nSPs properties for suppressing IL-18 or TSLP production might be value in the development of safer NMs.

On the other hands, we observed that only treated with nSP70 did not change pathology and local immune responses compared with PBS treated mouse except IL-18 productions (our preliminary data). However only IL-18 production was tendency to be enhanced by treatment with only silica nanoparticles, the enhancement of IL-18 productions are very slightly (not significant). Thus, we think the evoked inflammation in the ear was mainly attributed to the mixture of nSPs and Dp. Therefore we also must give attention to the interactions of nSPs with antigen to develop of safer NMs.

Conclusions

In this study, we showed the intradermal injections of SPs and Dp antigen aggravate AD-like skin lesions in size dependent manner. We speculated that particle size affects SPs-induced IL-18 and TSLP inductions enhance the Th2 immune responses related to Dp and then induce aggravation of AD-like skin lesions. On the other hands, the further studies are required to analyze the mechanisms why IL-18 and TSLP are induced by nSPs. Furthermore, the studies are also required to investigate whether SPs are the risk factor of AD using topical applications of SPs, which is a more likely mode of exposure to NMs. Considering the fact that the nSPs already used in general are smaller than our used ones, our results demand a careful hand. We consider that appropriate regulation of physical and chemical properties of nanoparticles, including sizes mediated by the inductions of IL-18 and TSLP are critical determinants for the design of safer forms of NMs.

Methods

SPs

Suspensions of SPs (Micromod Partikeltechnologie GmbH, Rostock, Germany) (25 and 50 mg ml^{-1} in water) were used; particle size diameters were 1000, 300, 100, 70, and 30 nm (designated as mSP1000, nSP300, nSP100, nSP70, and nSP30, respectively). These SPs don't have any coating. SP suspensions were stored at room temperature. The suspensions were sonicated in power of 400 W for 5 min at 25°C and then vortexed for 1 min immediately prior to use.

Mice

Male NC/Nga slc mice were purchased from Nippon SLC (Kyoto, Japan) and used at 8 weeks of age. We used n = 4 or 5 animals per each assay. All animal experimental procedures were performed in accordance with the institutional ethical guidelines for animal experiments.

Physicochemical examination of SPs

SPs were diluted to 0.25 mg ml^{-1} (nSP30 and nSP70) or 0.5 mg ml^{-1} (nSP100, nSP300, and mSP1000) with PBS (Sigma-Aldrich, St. Louis, MO, USA), and the average particle size and zeta potential were measured using a Zetasizer Nano-ZS (Malvern Instruments Ltd., Worcestershire, UK) at 25°C. The mean size and size distribution of SPs were measured using the dynamic light scattering method. The zeta potential was measured by laser Doppler electrophoresis. We perform these measurements using Size and Zeta capillary cell (Malvern Instruments Ltd). The pH of each particle suspension was measured with an ISFET pH meter (Shindengen, Tokyo, Japan).

Study protocols

Mice were divided into seven experimental groups (4 or 5 mice were used in each group): PBS, Dp, Dp + mSP1000, Dp + nSP300, Dp + nSP100, Dp + nSP70, and Dp + nSP30 groups. The PBS group received 20 μl of PBS. The Dp group received 2.5 μg of Dp mite allergen extract (Cosmo Bio LSL, Tokyo, Japan) in 20 μl PBS. The Dp + mSP1000, Dp + nSP300, Dp + nSP100, Dp + nSP70, and Dp + nSP30 groups received a combined administration of 2.5 μg Dp and 250 μg SPs (1000, 300, 100, 70, or 30 nm) in 20 μl PBS. Mice were intradermally injected on the ventral side of both their ears with Dp alone or Dp plus SPs in PBS on days 1, 3, 5, 7, 9, 11, 13, 16, and 18 under anesthesia with pentobarbital (somnopentyl; Kyouritsuseiyaku, Tokyo, Japan). The amount of injected liquid was 10 μl per ear. We measured ear thickness on days 0 and 19.

Histological analysis

At 24 h after the last intradermal injection, the ears of mice were removed and placed in fixative solution (4% paraformaldehyde in PBS; Wako, Osaka, Japan). A histopathological examination was performed by the Applied Medical Research Laboratory (AMRL; Osaka, Japan). Several representative symptoms (scab, acanthosis, inflammatory cell infiltration, and scleredema) observed in the AD of each sample were scored as 0 (none), 1 (very mild), 2 (mild), 3 (moderate), or 4 (severe). Scoring was also performed by AMRL, who was unaware of the treatment assignments. Mast cell numbers in three high-power fields at ×400 magnification were selected randomly and counted.

Blood sampling

Mice were anesthetized with pentobarbital 24 h after the last intradermal injection. The chest and abdominal walls were opened, and blood was sampled by cardiac puncture. Then blood was centrifuged at 3000 g at 4°C and we obtained plasma. Plasma was stored at -80°C until assay.

Quantitation of total IgE Abs

Total IgE in plasma was measured with an ELISA assay kit (BD Biosciences, San Diego, CA, USA) according to the manufacturer's instructions.

Detection of Dp-specific Ab by ELISA

Antigen-specific Ab levels in plasma were determined by ELISA. ELISA plates (Maxisorp, type 96F; Nunc A/S, Roskilde, Denmark) were coated with 100 μg ml^{-1} Dp in coating buffer PBS and incubated overnight at 4°C. The plates were washed with PBS-Tween20, incubated with blocking solution (Block Ace; Dainippon Sumitomo Pharmaceuticals, Osaka, Japan) at room temperature (RT) for 2 h, and plasma dilutions were added to the antigen-coated plates. After a 2-h RT incubation, the coated plates were washed with PBS-Tween20 and incubated with a HRP-conjugated goat anti-mouse IgG or IgG1 solution or a biotin-conjugated goat anti-mouse IgG2a or IgE detection Ab solution (Southern Biotechnology Associates, Birmingham, AL, USA) at RT for 2 h. To detect IgG2a or IgE, the plates were washed with PBS-Tween20 and then incubated with HRP-coupled streptavidin (Southern Biotechnology Associates) for 30 h at RT. After the incubation, the color reaction was developed with tetra methyl benzidine (MOSS, Inc.; Pasadena, MD, USA), stopped with 2 N H_2SO_4, and measured at $OD_{450\text{-}620}$ on a microplate reader.

Isolation of splenocytes

Spleens were aseptically removed and placed in RPMI 1640 (Wako) supplemented with 10% FBS, 10 ml L^{-1} of a 100 × nonessential amino acid solution (Gibco, Invitrogen, Carlsbad, CA, USA), 50 μM 2-mercaptoethanol (Gibco), and 1% antibiotic cocktail (Pennicilin; 10000 U/mL, Streptomycin; 10000 μg/mL, amphotericin B; 25 μg/mL) (Gibco). A single-cell suspension of splenocytes was treated with ammonium chloride to lyse the red blood cells, which were washed, counted, and suspended in RPMI 1640 to a final concentration of 1×10^7 cells ml^{-1}.

ELISPOT assay

An ELISPOT assay was performed to detect interferon (IFN)- γ and IL-4 producing cells. Dp-specific cytokine responses were evaluated by culturing the splenocytes (5×10^5 cells $well^{-1}$) stimulated with Dp (100 μg ml^{-1}) *in vitro*. After a 24-h incubation at 37°C, the plate was washed, and the IFN-γ- and IL-4-producing cells were measured with an ELISPOT assay kit (BD Biosciences) according to the manufacturer's instructions.

Quantitation of cytokine protein levels in ear tissue supernatants

At 24 h after the last intradermal injection, mice ears were removed and stored at -80°C. Later, the ears were homogenized with cell extraction buffer (Invitrogen). The homogenates were then centrifuged at 10,000 rpm for 5 min, and the supernatants were stored at -30°C. ELISAs for IFN-γ (BD Biosciences), IL-4, IL-5, IL-13 (eBioscience, San Diego, CA, USA), IL-18 (MBL, Nagoya, Japan), and thymic stromal lymphopoietin (TSLP; R&D Systems, Minneapolis, MN, USA) in the ear tissue supernatants were performed according to the manufacturer's instructions.

Statistical analysis

All data are presented as mean ± SE. The significant differences among groups were determined by ANOVA. Differences between the experimental groups and the control group were determined by Williams' test. $P < 0.05$ was considered significant.

Acknowledgements

This study was supported, in part, by Grants-in-Aid for Scientific Research from the Ministry of Education, Culture, Sports, Science and Technology of Japan (MEXT) and from the Japan Society for the Promotion of Science (JSPS); and by the Knowledge Cluster Initiative (MEXT); by Health Labour Sciences Research Grants from the Ministry of Health, Labour and Welfare of Japan (MHLW); by a Global Environment Research Fund from the Ministry of the Environment; by Food Safety Commission (Cabinet Office); by The Cosmetology Research Foundation; by The Smoking Research Foundation; and by The Takeda Science Foundation.

Author details

[1]Laboratory of Toxicology and Safety Science, Graduate School of Pharmaceutical Sciences, Osaka University, 1-6, Yamadaoka, Suita, Osaka 565-0871, Japan. [2]Laboratory of Biopharmaceutical Research (Pharmaceutical Proteomics), National Institute of Biomedical Innovation, 7-6-8, Saito-Asagi, Ibaraki, Osaka 567-0085, Japan. [3]The Center for Advanced Medical Engineering and Informatics, Osaka University, 1-6, Yamadaoka, Suita, Osaka 565-0871, Japan.

Authors' contributions

TH and TY designed the study; TH, HN, TY, S. Tochigi, KI, MU and TA performed experiments; TH and TY collected and analyzed data; TH and TY wrote the manuscript; KN, YA, YY, HK, NI and S. Tsunoda gave technical support and conceptual advice. YT supervised the all of projects. All authors discussed the results and commented on the manuscript. All authors have read and approved the final manuscript.

Competing interests

The authors declare that they have no competing interests.

Received: 21 September 2011 Accepted: 2 February 2012
Published: 2 February 2012

References

1. Bowman DM, van Calster G, Friedrichs S: **Nanomaterials and regulation of cosmetics.** *Nat Nanotechnol* 2010, **5**:92.
2. Liu D, Gu N: **Nanomaterials for fresh-keeping and sterilization in food preservation.** *Recent Pat Food Nutr Agric* 2009, **1**:149-154.
3. Salata O: **Applications of nanoparticles in biology and medicine.** *J Nanobiotechnology* 2004, **2**:3.
4. Choksi AN, Poonawalla T, Wilkerson MG: **Nanoparticles: a closer look at their dermal effects.** *J Drugs Dermatol* 2010, **9**:475-481.
5. Nel A, Xia T, Madler L, Li N: **Toxic potential of materials at the nanolevel.** *Science* 2006, **311**:622-627.
6. Shimizu M, Tainaka H, Oba T, Mizuo K, Umezawa M, Takeda K: **Maternal exposure to nanoparticulate titanium dioxide during the prenatal period alters gene expression related to brain development in the mouse.** *Part Fibre Toxicol* 2009, **6**:20.
7. Nishimori H, Kondoh M, Isoda K, Tsunoda S, Tsutsumi Y, Yagi K: **Silica nanoparticles as hepatotoxicants.** *Eur J Pharm Biopharm* 2009, **72**:496-501.
8. Yamashita K, Yoshioka Y, Higashisaka K, Mimura K, Morishita Y, Nozaki M, Yoshida T, Ogura T, Nabeshi H, Nagano K, *et al*: **Silica and titanium dioxide nanoparticles cause pregnancy complications in mice.** *Nat Nanotechnol* 2011, **6**:321-328.
9. Knopp D, Tang D, Niessner R: **Review: bioanalytical applications of biomolecule-functionalized nanometer-sized doped silica particles.** *Anal Chim Acta* 2009, **647**:14-30.
10. Martin KR: **The chemistry of silica and its potential health benefits.** *J Nutr Health Aging* 2007, **11**:94-97.
11. Nabeshi H, Yoshikawa T, Matsuyama K, Nakazato Y, Matsuo K, Arimori A, Isobe M, Tochigi S, Kondoh S, Hirai T, *et al*: **Systemic distribution, nuclear entry and cytotoxicity of amorphous nanosilica following topical application.** *Biomaterials* 2011, **32**:2713-2724.
12. Nabeshi H, Yoshikawa T, Matsuyama K, Nakazato Y, Arimori A, Isobe M, Tochigi S, Kondoh S, Hirai T, Akase T, *et al*: **Size-dependent cytotoxic effects of amorphous silica nanoparticles on Langerhans cells.** *Pharmazie* 2010, **65**:199-201.
13. Bohle B, Schwihla H, Hu HZ, Friedl-Hajek R, Sowka S, Ferreira F, Breiteneder H, Bruijnzeel-Koomen CA, de Weger RA, Mudde GC, *et al*: **Long-lived Th2 clones specific for seasonal and perennial allergens can be detected in blood and skin by their TCR-hypervariable regions.** *J Immunol* 1998, **160**:2022-2027.
14. Flohr C, Johansson SG, Wahlgren CF, Williams H: **How atopic is atopic dermatitis?** *J Allergy Clin Immunol* 2004, **114**:150-158.
15. Schafer T, Heinrich J, Wjst M, Adam H, Ring J, Wichmann HE: **Association between severity of atopic eczema and degree of sensitization to aeroallergens in schoolchildren.** *J Allergy Clin Immunol* 1999, **104**:1280-1284.
16. Bieber T: **Atopic dermatitis.** *Ann Dermatol* 2010, **22**:125-137.
17. Plotz SG, Ring J: **What's new in atopic eczema?** *Expert Opin Emerg Drugs* 2010, **15**:249-267.
18. Annesi-Maesano I, Caillaud D, Lavaud F, Moreau D, Le Moullec Y, Taytard A, Pauli G, Charpin D: **Exposure to fine air particles and occurrence of allergic diseases: results of ISAAC-France phase 2.** *Arch Pediatr* 2009, **16**:299-305.
19. Annesi-Maesano I, Moreau D, Caillaud D, Lavaud F, Le Moullec Y, Taytard A, Pauli G, Charpin D: **Residential proximity fine particles related to allergic sensitisation and asthma in primary school children.** *Respir Med* 2007, **101**:1721-1729.
20. Yanagisawa R, Takano H, Inoue K, Koike E, Kamachi T, Sadakane K, Ichinose T: **Titanium dioxide nanoparticles aggravate atopic dermatitis-like skin lesions in NC/Nga mice.** *Exp Biol Med (Maywood)* 2009, **234**:314-322.
21. Yanagisawa R, Takano H, Inoue KI, Koike E, Sadakane K, Ichinose T: **Size effects of polystyrene nanoparticles on atopic dermatitislike skin lesions in NC/NGA mice.** *Int J Immunopathol Pharmacol* 2010, **23**:131-141.
22. Kawakami T, Ando T, Kimura M, Wilson BS, Kawakami Y: **Mast cells in atopic dermatitis.** *Curr Opin Immunol* 2009, **21**:666-678.
23. Yamashita H, Michibata Y, Mizukami H, Ogihara Y, Morita A, Nose M: **Dermal mast cells play a central role in the incidence of scratching behavior in mice induced by multiple application of the hapten, 2,4,6-trinitrochlorobenzene.** *Exp Dermatol* 2005, **14**:438-444.
24. Stone KD, Prussin C, Metcalfe DD: **IgE, mast cells, basophils, and eosinophils.** *J Allergy Clin Immunol* 2010, **125**:S73-80.
25. Hirai T, Yoshikawa T, Nabeshi H, Yoshida T, Tochigi S, Uji M, Ichihashi K, Akase T, Yamashita T, Yamashita K, Nagano K, Abe Y, Kamada H, Tsunoda S, Yoshioka Y, Itoh N, Tsutsumi Y: **Size-dependent immune-modulating effect of amorphous nanosilica particles.** *Pharmazie* .
26. Tran KK, Shen H: **The role of phagosomal pH on the size-dependent efficiency of cross-presentation by dendritic cells.** *Biomaterials* 2009, **30**:1356-1362.

27. Aral M, Arican O, Gul M, Sasmaz S, Kocturk SA, Kastal U, Ekerbicer HC: **The relationship between serum levels of total IgE, IL-18, IL-12, IFN-gamma and disease severity in children with atopic dermatitis.** *Mediators Inflamm* 2006, **2006**:73098.
28. Hon KL, Lam MC, Leung TF, Wong KY, Chow CM, Fok TF, Ng PC: **Are age-specific high serum IgE levels associated with worse symptomatology in children with atopic dermatitis?** *Int J Dermatol* 2007, **46**:1258-1262.
29. Kay AB, Ying S, Varney V, Gaga M, Durham SR, Moqbel R, Wardlaw AJ, Hamid Q: **Messenger RNA expression of the cytokine gene cluster, interleukin 3 (IL-3), IL-4, IL-5, and granulocyte/macrophage colony-stimulating factor, in allergen-induced late-phase cutaneous reactions in atopic subjects.** *J Exp Med* 1991, **173**:775-778.
30. Rousset F, Robert J, Andary M, Bonnin JP, Souillet G, Chretien I, Briere F, Pene J, de Vries JE: **Shifts in interleukin-4 and interferon-gamma production by T cells of patients with elevated serum IgE levels and the modulatory effects of these lymphokines on spontaneous IgE synthesis.** *J Allergy Clin Immunol* 1991, **87**:58-69.
31. Leung DY, Boguniewicz M, Howell MD, Nomura I, Hamid QA: **New insights into atopic dermatitis.** *J Clin Invest* 2004, **113**:651-657.
32. Liu FT, Goodarzi H, Chen HY: **IgE, Mast Cells, and Eosinophils in Atopic Dermatitis.** *Clin Rev Allergy Immunol* 2011.
33. Elias PM, Steinhoff M: **"Outside-to-inside" (and now back to "outside") pathogenic mechanisms in atopic dermatitis.** *J Invest Dermatol* 2008, **128**:1067-1070.
34. Konishi H, Tsutsui H, Murakami T, Yumikura-Futatsugi S, Yamanaka K, Tanaka M, Iwakura Y, Suzuki N, Takeda K, Akira S, *et al*: **IL-18 contributes to the spontaneous development of atopic dermatitis-like inflammatory skin lesion independently of IgE/stat6 under specific pathogen-free conditions.** *Proc Natl Acad Sci USA* 2002, **99**:11340-11345.
35. Ziegler SF, Artis D: **Sensing the outside world: TSLP regulates barrier immunity.** *Nat Immunol* 2010, **11**:289-293.
36. Terada M, Tsutsui H, Imai Y, Yasuda K, Mizutani H, Yamanishi K, Kubo M, Matsui K, Sano H, Nakanishi K: **Contribution of IL-18 to atopic-dermatitis-like skin inflammation induced by Staphylococcus aureus product in mice.** *Proc Natl Acad Sci USA* 2006, **103**:8816-8821.
37. Yoshimoto T, Min B, Sugimoto T, Hayashi N, Ishikawa Y, Sasaki Y, Hata H, Takeda K, Okumura K, Van Kaer L, *et al*: **Nonredundant roles for CD1d-restricted natural killer T cells and conventional CD4+ T cells in the induction of immunoglobulin E antibodies in response to interleukin 18 treatment of mice.** *J Exp Med* 2003, **197**:997-1005.
38. Yoshimoto T, Nakanishi K: **Roles of IL-18 in basophils and mast cells.** *Allergol Int* 2006, **55**:105-113.
39. Yoshimoto T, Tsutsui H, Tominaga K, Hoshino K, Okamura H, Akira S, Paul WE, Nakanishi K: **IL-18, although antiallergic when administered with IL-12, stimulates IL-4 and histamine release by basophils.** *Proc Natl Acad Sci USA* 1999, **96**:13962-13966.
40. Fang C, Siew LQ, Corrigan CJ, Ying S: **The role of thymic stromal lymphopoietin in allergic inflammation and chronic obstructive pulmonary disease.** *Arch Immunol Ther Exp (Warsz)* 2010, **58**:81-90.

doi:10.1186/1743-8977-9-3
Cite this article as: Hirai *et al.*: Amorphous silica nanoparticles size-dependently aggravate atopic dermatitis-like skin lesions following an intradermal injection. *Particle and Fibre Toxicology* 2012 **9**:3.

Amorphous nanosilicas induce consumptive coagulopathy after systemic exposure

2012 Nanotechnology 23 045101

(http://iopscience.iop.org/0957-4484/23/4/045101)

IOP PUBLISHING NANOTECHNOLOGY
Nanotechnology **23** (2012) 045101 (8pp) doi:10.1088/0957-4484/23/4/045101

Amorphous nanosilicas induce consumptive coagulopathy after systemic exposure

Hiromi Nabeshi[1,2,8], Tomoaki Yoshikawa[1,2,8,9], Keigo Matsuyama[1,2], Yasutaro Nakazato[1,2], Akihiro Arimori[1,2], Masaaki Isobe[1,2], Saeko Tochigi[1,2], Sayuri Kondoh[1,2], Toshiro Hirai[1,2], Takanori Akase[1,2], Takuya Yamashita[1,2], Kohei Yamashita[1,2], Tokuyuki Yoshida[1,2], Kazuya Nagano[2], Yasuhiro Abe[2], Yasuo Yoshioka[2,3], Haruhiko Kamada[2,3], Takayoshi Imazawa[4], Norio Itoh[1,2], Masuo Kondoh[5], Kiyohito Yagi[5], Tadanori Mayumi[6], Shin-ichi Tsunoda[2,3,7] and Yasuo Tsutsumi[1,2,3,9]

[1] Laboratory of Toxicology and Safety Science, Graduate School of Pharmaceutical Sciences, Osaka University, 1-6 Yamadaoka, Suita, Osaka, 565-0871, Japan
[2] Laboratory of Biopharmaceutical Research (Pharmaceutical Proteomics), National Institute of Biomedical Innovation, 7-6-8 Saito-Asagi, Ibaraki, Osaka, 567-0085, Japan
[3] The Center for Advanced Medical Engineering and Informatics, Osaka University, 1-6 Yamadaoka, Suita, Osaka, 565-0871, Japan
[4] Bioresources Research, Laboratory of Common Apparatus, National Institute of Biomedical Innovation, 7-6-8 Saito-Asagi, Ibaraki, Osaka, 567-0085, Japan
[5] Laboratory of Bio-Functional Molecular Chemistry, Graduate School of Pharmaceutical Sciences, Osaka University, 1-6 Yamadaoka, Suita, Osaka, 565-0871, Japan
[6] Graduate School of Pharmaceutical Sciences, Kobe-Gakuin University, 1-1-3 Minatojima, Chuo-ku, Kobe, Hyogo, 650-8586, Japan
[7] Laboratory of Biomedical Innovation, Graduate School of Pharmaceutical Sciences, Osaka University, 7-6-8 Saito-Asagi, Ibaraki, Osaka, 567-0085, Japan
E-mail: tomoaki@phs.osaka-u.ac.jp and ytsutsumi@phs.osaka-u.ac.jp

Received 11 September 2011, in final form 11 November 2011
Published 4 January 2012
Online at stacks.iop.org/Nano/23/045101

Abstract
We previously reported that well-dispersed amorphous nanosilicas with particle size 70 nm (nSP70) penetrate skin and produce systemic exposure after topical application. These findings underscore the need to examine biological effects after systemic exposure to nanosilicas. The present study was designed to examine the biological effects. BALB/c mice were intravenously injected with amorphous nanosilicas of sizes 70, 100, 300, 1000 nm and then assessed for survival, blood biochemistry, and coagulation. As a result, injection of nSP70 caused fatal toxicity, liver damage, and platelet depletion, suggesting that nSP70 caused consumptive coagulopathy. Additionally, nSP70 exerts procoagulant activity *in vitro* associated with an increase in specific surface area, which increases as diameter reduces. In contrast, nSP70-mediated procoagulant activity was absent in factor XII-deficient plasma. Collectively, we revealed that interaction between nSP70 and intrinsic coagulation factors such as factor XII, were deeply related to nSP70-induced harmful effects. In other words, it is suggested that if interaction between nSP70 and coagulation factors can be suppressed, nSP70-induced harmful effects may be avoided. These results would provide useful

[8] These authors contributed equally to the work.
[9] Address for correspondence: Laboratory of Toxicology and Safety Science, Graduate School of Pharmaceutical Sciences, Osaka University, 1-6 Yamadaoka, Suita, Osaka 565-0871, Japan.

information for ensuring the safety of nanomaterials (NMs) and open new frontiers in biological fields by the use of NMs.

(Some figures may appear in colour only in the online journal)

1. Introduction

Synthetically produced amorphous silicon dioxide (silica) is intentionally manufactured as a nanometer sized material. Amorphous nanosilica particle (nSP) production exceeds 1 M tons per year and the market is estimated at $3.14 billion; quantities of nSPs consumed are among the largest of any nanomaterials (NMs) available commercially [1]. nSPs are used for anti-caking and flow improvement in common salt and food powders such as spray-dried vegetables, fruits, eggs, and coffee creamers, as a thickening or stabilizing agent in emulsions (both in foods and cosmetics) [2], to achieve viscosity and transparency in oils for cosmetics, or to improve storage and temperature stability. They are also used to improve free-flowing properties of hair bleaching agents and coating performance in nail polishes, and for distributing pigments in lipsticks and make-up [3, 4]. Furthermore, nSPs also have great potential for use as diagnostic imaging agents, gene delivery carriers, and cancer therapies [5–9]. In recent years, the ability to decrease nSP size has made progress at an accelerated rate, since the more size decreases, the more useful functions such as colorlessness and anti-caking increase. nSPs of 2.5 nm in size can now be generated. In fact, although nSPs have dramatically different properties from bulk sized silica particles, their safety remains unknown. However, it is no exaggeration to state that the types of application, amount of production, and opportunity for exposure of humans to nSPs are overwhelmingly large. Furthermore, because nSPs have received a lot of attention as gene delivery carrier and/or contrast agent candidates in recent years, opportunity for exposure of humans to nSPs is expected to increase further in the near future. Therefore, it is an urgent and necessary issue to elucidate the biological effects of nSPs for safety use to humans.

In a previous study, we reported that well-dispersed nSPs and quantum dots (QDs) of less than 100 nm in a diameter penetrate the skin barrier, produce systemic exposure, and can reach the brain, liver and regional lymph nodes [10]. This fact suggests the possibility that exposure to nSPs in cosmetics and/or foods poses an unknown risk not only to the application area but also the whole body. In addition, we revealed that nSPs could cause pregnancy complications when injected intravenously into pregnant mice [11], and generate intracellular reactive oxygen species (ROS) *in vitro* [12], although larger silica particles did not cause this toxicity. However, because the information on biological effects of NMs is not enough yet, it is necessary to clarify the nature of *in vivo* acute toxicity and possible mechanisms for ensuring the safety of NMs. In this study, we decided to examine acute toxicity of silica particles with sizes of 70, 100, 300, and 1000 nm (designated nSP70, nSP100, nSP300, and mSP1000 respectively), and QDs of 35 nm after intravenous injection. In this study, we have investigated the *in vivo* distribution toxicity of nSP after intravenous injection, which is useful for ensuring the safety of NMs.

2. Materials and methods

2.1. Silica particles

Fluorescent (red-F)-labeled amorphous silica particle suspensions (25 or 50 mg ml^{-1}) with diameters of 70, 100, 300, and 1000 nm (Micromod Partikeltechnologie GmbH; designated nSP70, nSP100, nSP300, and mSP1000, respectively) were used in this study. Silica particles were used after 5 min sonication and 1 min vortexing. Physicochemical information about these silica particles has been described in our previous reports [10, 12].

2.2. Quantum dots

QDs with emission maxima at 565 nm were obtained from Invitrogen (Hayward, CA). They were sold as Qtracker® Non-targeted Quantum Dots (PEG). QDs were used after 5 min sonication and 1 min vortexing.

2.3. Animals

BALB/c mice (female, 6–8 weeks) were purchased from Japan SLC, Inc. The mice were housed in a ventilated animal room maintained at 20±2 °C with a 12 h light/12 h dark cycle. Mice had free access to water and forage (FR-2, Funabashi farm). The experimental protocols conformed to the ethical guidelines of the National Institute of Biomedical Innovation.

2.4. Acute lethal toxicity test

BALB/c mice were administered silica particle samples by bolus injection at a dose of 2 mg $mouse^{-1}$ (about 100 mg kg^{-1}) and their survival followed up for 24 h. To calculate the lethal dose 50% (LD50) of nSP70, various concentrations of nSP70 were injected intravenously.

2.5. Blood sample collection

Eight female BALB/c mice were treated with 2 mg $mouse^{-1}$ (about 100 mg kg^{-1}) silica particles of each particle size (70, 100, 300, and 1000 nm) and PBS (control) by intravenous injection. After 1, 5, or 6 h, blood samples were collected from the heart using plastic syringes (TERUMO) containing 1/9 volume of 3.8% sodium citrate (for hepaplastin test) or wetting with 5 IU ml^{-1} heparin sodium (for biomarker assay). Plasma was harvested by centrifuging blood at 1750*g* for 10 min.

2.6. Blood biomarker assay

Liver function was evaluated by measuring plasma levels of alanine aminotransferase (ALT), aspartate aminotransferase (AST), gamma-glutamyltransferase (GGT), lactate dehydrogenase (LDH), albumin (ALB), total cholesterol (TCHO), total bilirubin (TBIL), and ammonia (NH_3). Nephrotoxicity was determined from blood urea nitrogen (BUN). All assays were carried out using a biochemical auto-analyzer (FUJI DRI-CHEM 7000; FUJIFILM).

2.7. Isolation of primary hepatocytes from silica particle-treated mice

Female BALB/c mice were treated with 2 mg mouse^{-1} (about 100 mg kg^{-1}) silica particles of each particle size (70, 100, 300, and 1000 nm) and PBS (control) by intravenous injection. After 5 h, parenchymal hepatocytes were isolated according to the *in situ* two-step collagenase perfusion technique. Briefly, the liver was perfused with 25 ml of 10 mM Hepes buffered calcium- and magnesium-free Hanks' balanced salt solution (HBSS) containing 190 mg l^{-1} EGTA (DOJINDO) for 5 min. The liver was then perfused with 40 ml of HBSS containing 250 mg l^{-1} trypsin inhibitor, 500 mg l^{-1} collagenase, and 550 mg l^{-1} $CaCl_2$ for 10 min. The liver was then excised and the cells dispersed in HBSS. The cells were then centrifuged at 50*g* at 4 °C for 1 min. The resulting pellet was resuspended in 20 ml of L15 medium containing 5% FCS, 1 μM dexamethasone and 1 μM insulin and centrifuged at 50*g* at 4 °C for 1 min. This step was repeated three times. The resulting pellet was resuspended in medium at a concentration of 1.0×10^5 living cells ml^{-1}.

2.8. Hepaplastin test

The hepaplastin test were carried out using the hepaplastin test® kit (Sanko Junyaku Co., Ltd) for humans. 250 μl of hepaplastin regent were put into a plastic tube and incubated at 37 °C for 3 min. Then, 15 μl of plasma, collected from silica particle-treated mice, was added to the plastic tube and the coagulation time was measured at 37 °C. Hepaplastin values were calculated using the correlation table attached to the kit.

2.9. Histopathological examination

Three female BALB/c mice were treated with 2 mg mouse^{-1} (about 100 mg kg^{-1}) silica particles of each particle size (70, 300, and 1000 nm) and PBS (control) by intravenous injection. After 6 h, the tissues and organs such as brain, heart, lung, liver, kidney, spleen, and lymph node, were excised and fixed immediately in 4% paraformaldehyde. The tissues were embedded in paraffin blocks, then sliced and placed on glass slides. After hematoxylin–eosin (HE) staining, the slides were observed and scored by 5 grades (0: none, 1: very slight, 2: mild, 3: moderate, 4: advanced). The protocol following tissue fixing and the evaluation of pathological images complied with the Applied Medical Research Laboratory.

2.10. Vascular permeability

After 1 h treatment with silica particles, BALB/c mice were injected intravenously with 2% Evans Blue at 4 ml kg^{-1}. After a further 30 min, ear color was observed and photographed.

2.11. Hematology analysis

Whole blood was collected 5 h after administration of silica particles and was analyzed for the number of white blood cells, lymphocytes, monocytes, granulocytes, red blood cells, and platelets, as well as amounts of hemoglobin and the rate of hematocrit using an auto-analyzer, VetScan HMII Hematology System (Abaxis).

2.12. Coagulation tests

BALB/c mice were treated with 2 mg mouse^{-1} (about 100 mg kg^{-1}) silica particles of each particle size (70, 300, and 1000 nm) and PBS (control) by intravenous injection. As the blood coagulation positive control, mice were treated with 5 mg kg^{-1} LPS (*Escherichia coli*, serotype 055:B5, SIGMA) by intravenous injection. After 5 h, blood was withdrawn from the heart into a plastic syringe containing 1/9 volume of 3.8% sodium citrate and the coagulation tests were performed with plasma separated from the blood by centrifugation (1750*g* for 10 min at 4 °C). Activated partial thromboplastin time (APTT) and prothrombin time (PT) were determined at 37 °C in the CLOTEK system (Hyland Division, Travenol Laboratories, Inc.) with APTT and PT reagents (Sysmex), respectively.

2.13. Survival of nSP70-injected mice with or without anticoagulant

Two minutes prior to nSP70 treatment (2 mg mouse^{-1} (about 100 mg kg^{-1})), the BALB/c mice were infused through the tail vein as a bolus with either PBS (vehicle) or anticoagulant heparin at doses of 5000 IU kg^{-1} and their survival followed up for 24 h.

2.14. In vitro silica clotting time

Venous blood was collected from healthy human volunteers in plastic tubes containing 1/9 volume of 3.8% sodium citrate and centrifuged at 1750*g* for 10 min at 4 °C. Factor XII-deficient plasma was purchased from Hematologic Technologies, Inc. (Essex Junction). One hundred μl of plasma and 100 μl of various sized silica particles (0.02 mg ml^{-1}) were mixed. After 3 min incubation at 37 °C, the resulting mixture was recalcified with 100 μl of 20 mM $CaCl_2$ and clotting time was recorded using the CLOTEK system.

2.15. Statistical analysis

Statistical comparisons between groups were performed by one-way ANOVA with the Bonferroni test as a *post hoc* test. The significance level was set at $P < 0.01$.

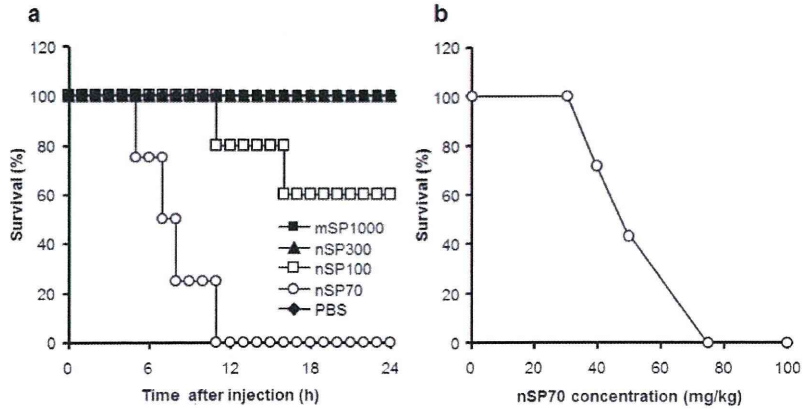

Figure 1. Survival curves of mice injected with different sized silica particles. (a) Acute toxicity in BALB/c mice (female, $n = 4$ or 5) injected intravenously with 2 mg mouse^{-1} silica particles (nSP70, 100, 300, and mSP1000) or PBS (control) was monitored for 24 h after injection. (b) Survival of BALB/c mice injected intravenously with 0.6, 0.8, 1.0, 1.5, and 2 mg mouse^{-1} nSP70 or PBS (0 mg kg^{-1}) for 48 h after injection. LD50 of nSP70 was calculated to be approximately 45 mg kg^{-1}.

3. Results and discussion

To elucidate the influence of the biological response of silica particles and QDs after passage into the bloodstream, we performed an acute lethal toxicity test using silica particles- or QD-injected mice intravenously. The result of survival evaluation showed that no lethal toxicity was observed in nSP300-, mSP1000-treated groups (2 mg mouse^{-1} (about 100 mg kg^{-1})). In contrast, 40% and all mice died in the nSP100- and nSP70-treated groups, respectively (figure 1(a)). The survival of nSP70-treated mice was decreased in a dose-dependent manner (figure 1(b)) and the lethal dose 50% (LD50) value of nSP70 was about 45 mg kg^{-1}. On the other hand, in the case of QD treatment, no lethal toxicity was observed at all. Therefore, the emergence of lethal toxicity would be dependent on both particle size and material effect because only the 100 nm or less size nSP shows lethal effects. Furthermore, the biological effects of NMs of less than 100 nm in diameter were not always determined by its diameter, suggesting that biological effects of NMs are associated with its complex physicochemical properties such as size, and surface character and its kinetics properties.

We previously reported that nSP70 entered the circulation, reached the liver, and induced DNA damage [10]; therefore, acute toxicity tests were next assessed. Biochemical examination of plasma (figure 2) showed that activity of the sensitive indicators of liver injury, aspartate aminotransferase (AST; figure 2(a)), alanine aminotransferase (ALT; figure 2(b)), and lactate dehydrogenase (LDH; figure 2(c)), increased significantly at and below the threshold particle size of 100 nm and these values reached abnormal levels. Albumin (ALB; figure 2(d) and total cholesterol (TCHO; figure 2(e)), which are indicators of liver function, showed the tendency to decrease in the nSP70-treated group compared with the other group. Total bilirubin (TBIL; figure 2(f)), an indicator of hepatobiliary system damage, was also increased significantly. Furthermore, our unpublished data indicated that serum inflammatory cytokine levels (TNF-α and IL-6) increased after intravenous injection of nSP70 (data not shown). We also revealed that hepaplastin values, indicators of the production of coagulation factor (factor II, VII, and X) in hepatocyte, were decreased in the nSP70-treated group compared with the other groups (figure 2(g)). These results suggested that nSP70 may induce the dysfunction of hepatocytes. In summary, these results indicate that differences in biological effects such as acute toxicity and liver toxicity are caused by differences in the biodistribution of silica particles. Additionally, preliminary data suggest that indications of hepatic inflammation such as the presence of minor granulation and a fibril formation were induced in mouse liver with frequent intravenous administration (data not shown). This result indicated that chronic exposure to nSP70 may increase the risk of hepatic cirrhosis or hepatic cancer.

As reported above, nSPs with particle size less than 100 nm can penetrate the skin barrier, distribute throughout the body, and induce liver toxicity. We next examined the mechanism responsible for the acute toxicity and liver toxicity. Firstly, we observed pathological liver sections and intense congestion of liver and spleen (figure 3) was seen in the nSP70-treated group. This suggests that nSP70 treatment leads to a disorder of blood coagulation. In fact, a vascular permeability test using Evans blue showed that the color of limbs, ears and nose were dramatically changed to blue in the group treated with nSP where particle size was less than 100 nm (figure 4(a)–(d)). Furthermore, the dramatic decrease in platelet count (figure 4(e)) and the abnormality of intrinsic/extrinsic coagulation (figures 4(f) and (g)) were observed only in the nSP70-treated group. These findings suggest that abnormal activation of the coagulation system following nSP70 administration may result in the depletion of coagulation factors, and the increase of vascular permeability. Based on these results, since we considered that the coagulation abnormality was contributing to lethal toxicity, we decided to examine the survival rates of nSP70-injected mice pretreated with the anticoagulant, heparin. Results showed that heparin treatment reduced the

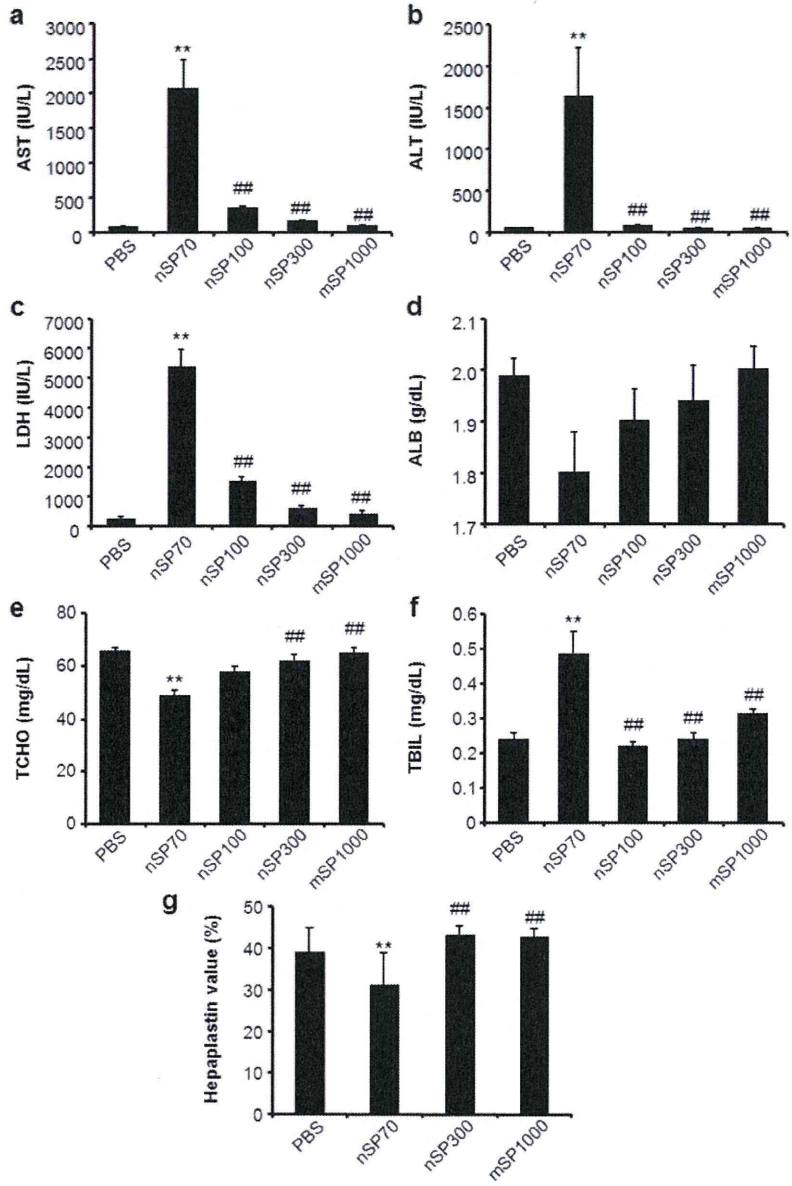

Figure 2. Liver toxicity analysis in silica particle-injected mice. (a)–(f) Measurement of biochemical parameters. Blood samples from BALB/c mice injected intravenously with 100 mg kg^{-1} silica particles (nSP70, 100, 300, and mSP1000) or PBS (control) were collected from the hearts 6 h after injection. Plasma was recovered by centrifugation of blood at 1750*g* for 10 min. Biochemical parameters were analyzed using Fuji Dri-Chem 7000 and the results are expressed as mean ± S.E. ($n = 8$). (g) Measurement of hepaplastin value. Coagulation times were measured using silica particle-treated mice plasma. Hepaplastin values were calculated using the correlation table attached to the hepaplastin test kit. ** represents a significant difference from the control group ($P < 0.01$). ## Represents a significant difference from the nSP70 group ($P < 0.01$).

acute toxicity induced by nSP70 treatment (figure 4(h)). This result demonstrated that acute fatal toxicity by nSP70 is initiated at the level of blood coagulation.

To clarify the causal factor of nSP70-mediated procoagulant activity, we next performed *in vitro* coagulation tests using human plasma. While normal human plasma to which nSP300 or mSP1000 was added clotted within approximately 180–200 s, nSP70-treated plasma clotted after 150 s (figure 5(a)). It is well known that contact activation of coagulation factor XII (FXII, Hageman factor) is one of the main causes of blood coagulation [13–16]. Activated FXII arises from its contact with hydrophilic activating particles (such as fully water-wettable glass) [17–20]. It is known that nanoparticles have the potential to induce different functions from micro-sized particles by quantum effects [21–23]. In the case of nSPs, Rahman *et al* reported that the specific area and the surface silanol group concentration of particles increased according to the particle size decrease [24]. This information, combined with our results suggests that the procoagulant activity of nSP70 was associated with the

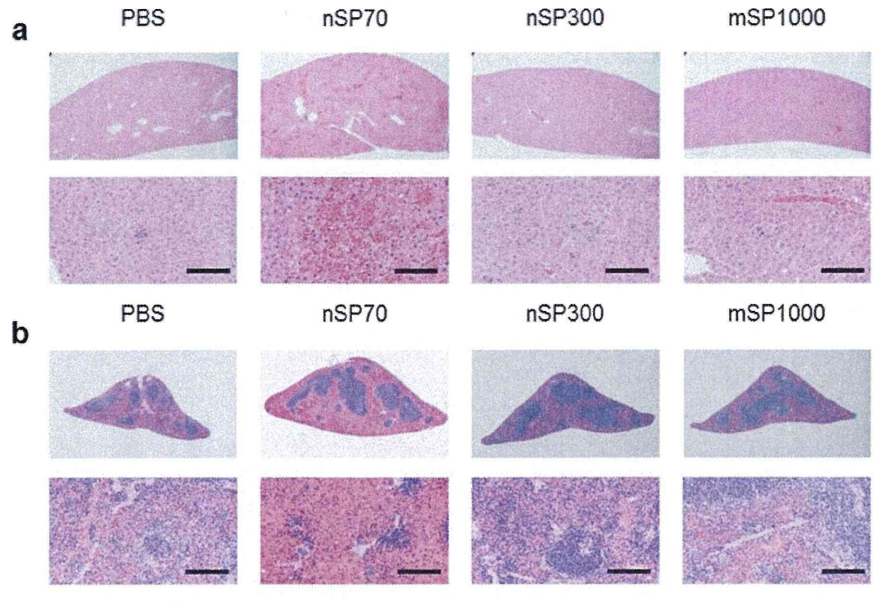

c

	Liver				Spleen
	inflammatory cell infiltration	vacuolization	single cell necrosis	congestion	congestion
Control	0.67 ± 0.33	2.0	0	0	0
nSP70	1.0 ± 0.41	2.25 ± 0.25	0.75 ± 0.25	2.5 ± 0.96	2.25 ± 0.75
nSP300	2.0	1.67 ± 0.33	0.33 ± 0.33	0	0.33 ± 0.33
mSP1000	1.33 ± 0.33	1.33 ± 0.33	0	0	0.67 ± 0.33

Figure 3. Histopathological analysis of liver and spleen in mice injected with silica particles. Liver (a) and spleen (b) in BALB/c mice injected with 100 mg kg^{-1} silica particles (nSP70, 300, and mSP1000) or PBS (control) were stained with hematoxylin–eosin (HE). Significant congestion was observed in the liver and spleen only in nSP70-treated mice. Scale bar: 100 μm. (c) Histopathological grades of heart, liver, and spleen are summarized. Grade; 0: none, 1: very slight, 2: mild, 3: moderate, 4: advanced. Results are expressed as mean of grade ± S.E. ($n = 3$).

increase of specific surface area and silanol group of this particle. In addition, because the numbers of the particles per weight were also increased according to particle size decrease, it was considered that contact opportunities between nSPs and FXII could be increased. As a result, blood coagulation might be accelerated. In fact, nSP70-mediated procoagulant activity was progressively decreased in the presence of increasing amounts of FXII-deficient plasma (figure 5(b)). Collectively, our results suggest that (1) the main causal factor of nSP70-mediated fatal toxicity was blood coagulation caused by nSP70 as a starting point, (2) interaction of nSP70 with FXII is critical to the production of its biological effects. Additionally, it is suspected that nSP70 has the potential to activate high molecular kininogen and prekallikrein; these molecules play the activation role of an intrinsic coagulation reaction as well as FXII [25]. On the other hand, because nSP70 induced high cytotoxicity and tissue damage compared to nSP300 and mSP1000 [10], nSP70 has the potential to induce damage to vascular endothelial cells followed by expression of tissue factor, which is known as the initiator of the extrinsic coagulation reaction [25]. Therefore, we think that nSP-induced effects on intrinsic and extrinsic coagulation need to be investigated further. Our study revealed that nSP70 accumulated in parenchymal hepatocytes at a high rate after intravenous injection, while nSP300 and mSP1000 tended to be trapped within Kupffer cells. Because the hepatocyte is a cell that manufactures fibrinogen and clotting factors [26–30], accumulation of nSP70 may reduce the production of clotting factors and affect the blood's ability to clot. Thus, the nSP70-induced clotting abnormality was induced by contact activation of FXII as well as dysfunction of the parenchymal hepatocyte.

In summary, these findings have revealed that the emergence of acute toxicity would be dependent on both particle size and material effect because only nSP shows the acute toxicity and nSP with sizes less than 100 nm, such as nSP70 and nSP100, differ from bulk materials with particle sizes above the nanoscale (100 nm) in terms of acute toxicity, liver toxicity, and *in vivo* distribution. In addition, the biophysicochemical interaction between nSP70s and FXII was important for bioadverse outcomes, such as consumptive coagulopathy. Most recently, we suggested that physicochemical properties of nSPs such as surface modification could alter the biological effects even if particle

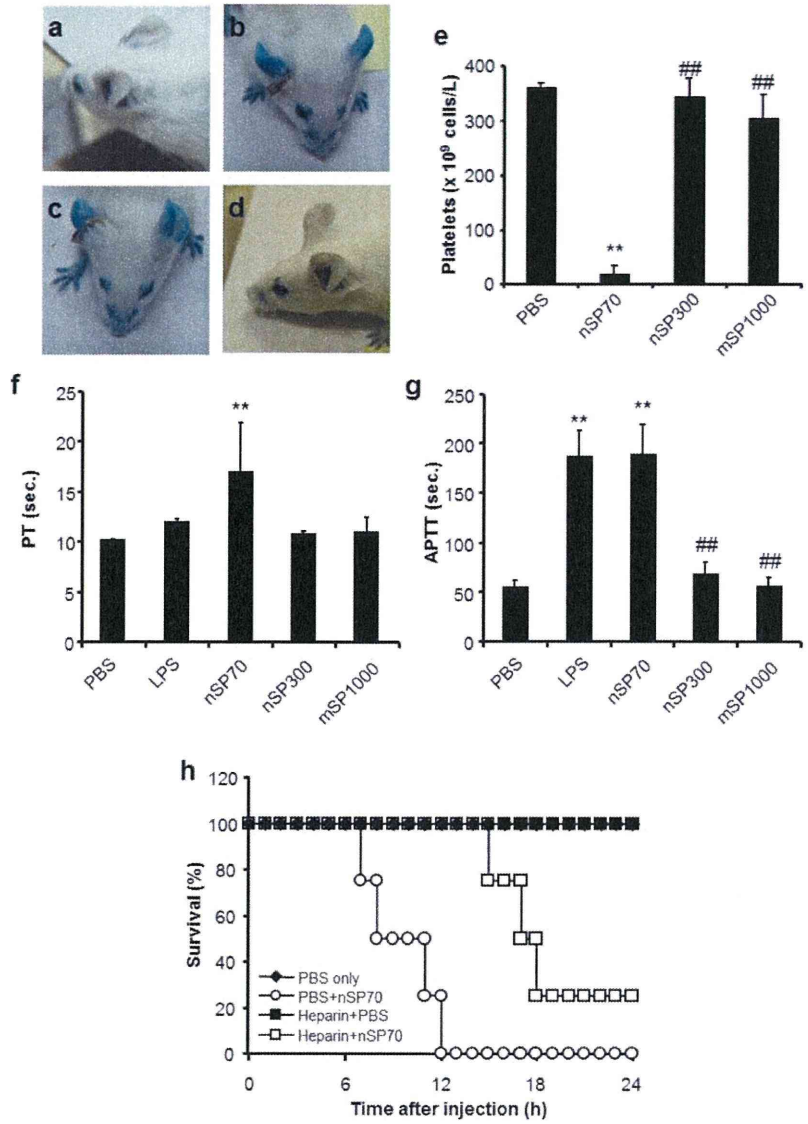

Figure 4. Blood coagulation analysis in mice injected with silica particles. (a)–(d) Influence of nSPs on microvascular leakage in BALB/c mouse skin. Photograph of mouse treated with PBS (a), nSP70 (b), nSP100 (c), or nSP300 (d) 90 min after treatment. Evans Blue extravasations were observed only in nSP70 and nSP100-treated mice. (e) Hematology analysis in whole blood of mice injected with silica particles. Blood samples from BALB/c mice injected intravenously with 100 mg kg^{-1} silica particles (nSP70, 300, and mSP1000) or PBS (control) were collected from heart 5 h after injection. Hematology analysis was performed using VetScan. Results are expressed as mean ± S.E. ($n = 3$). (f), (g) Coagulation response of the plasma of silica particle-injected mice. Plasma samples were collected from BALB/c mice injected with 100 mg kg^{-1} silica particles (nSP70, 300, and mSP1000), LPS (positive control), or PBS (control) 5 h after injection. Plasma was then assayed for PT (f) and APTT (g) by standard methods. Results are expressed as mean ± S.E. ($n = 3$). (h) The protective effect of anticoagulant on nSP70-induced lethal toxicity. 100 IU/mouse heparin or PBS (vehicle) was administrated by intravenous injection 2 min before nSP70 or PBS (control) injection. Survival was monitored for 24 h after injection. ** represents significant difference from the control ($P < 0.01$), ## represents significant difference from the nSP70 group ($P < 0.01$).

size was the same [31]. Although the mechanism of this finding is unclear, we speculate that one of the mechanisms is the change of interaction between nSPs and biological molecules such as protein induced by the surface properties of nSPs. Therefore, our current studies focus on analyzing biological interactions that nanoparticles may encounter in tissue culture medium, and following the interactions with cells (membranes, endosomes, organelles, and cytoplasm) or concomitantly administered drugs and foods.

4. Conclusions

We reveal here that the emergence of acute toxicity of nSPs would be dependent on both particle size and material effect such as the difference of blood coagulation activity and distribution behavior. These results suggest the importance of risk management of nSPs and the need for more information of nSPs' safety. We are now examining in detail the biological responses, biodistribution, and biological interactions which

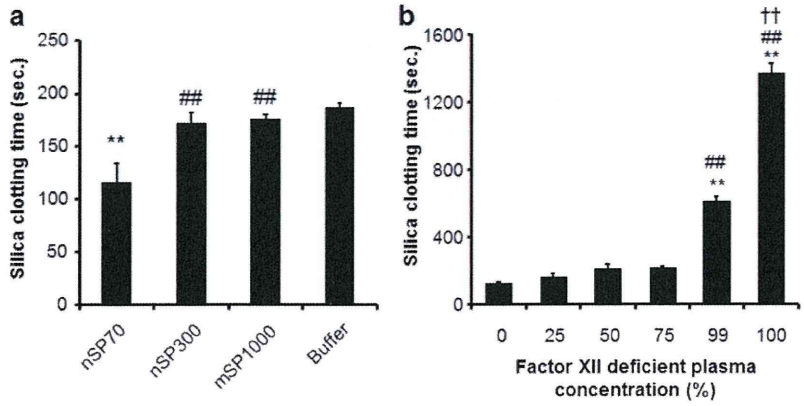

Figure 5. Measurement of the blood clotting time and the factor XII activation rate by silica particles *in vitro*. (a) Changes in silica clotting time with different sized silica particles (0.02 mg ml^{-1}) in healthy human plasma. Results are expressed as mean ± S.D. ($n = 3$). ** represents a significant difference from the buffer group ($P < 0.01$), ## represents a significant difference from the nSP70 group ($P < 0.01$). (b) *In vitro* silica clotting time measurement using mixtures of healthy and factor XII-deficient human plasma in various proportions. Silica clotting time was measured with nSP70 (0.02 mg ml^{-1}) using normal healthy plasma mixed with different amounts of coagulant factor XII-deficient human plasma (0 (healthy human plasma alone), 25, 50, 75, 99, and 100% (coagulant factor XII-deficient human plasma alone)). Results are expressed as mean ± S.D. ($n = 3$). ** represents a significant difference from 0% factor XII-deficient human plasma ($P < 0.01$), ## represents a significant difference from 25, 50, and 75% factor XII-deficient human plasma ($P < 0.01$), †† represents a significant difference from 99% factor XII-deficient human plasma ($P < 0.01$).

are linked to the physicochemical properties of NMs. We believe that the knowledge obtained from this research may constitute useful information for ensuring the safety of NMs.

Acknowledgments

This study was supported in part by Grants-in-Aid for Scientific Research from the Ministry of Education, Culture, Sports, Science, and Technology of Japan (MEXT), the Japan Society for the Promotion of Science (JSPS), the Knowledge Cluster Initiative (MEXT), and by Health Labour Sciences Research Grants from the Ministry of Health, Labor, and Welfare of Japan (MHLW), by a Global Environment Research Fund from the Minister of the Environment, by the Food Safety Commission (Cabinet Office), by The Cosmetology Research Foundation, by The Smoking Research Foundation, and by The Takeda Science Foundation.

References

[1] Royal Commission on Environmental Pollution 2008 *Novel Materials in the Environment: the Case of Nanotechnology* (London: Royal Commission) www.official-documents.gov.uk/document/cm74/7468/7468.pdf
[2] Merget R, Bauer T, Kupper H U, Philippou S, Bauer H D, Breitstadt R and Bruening T 2002 *Arch. Toxicol.* **75** 625
[3] Evonik 2008 Evonik, Documents on Aerosil [online] www.aerosil.com/aerosil/en/industries/food/default www.aerosil.com/aerosil/en/industries/personalcare/skincare/default www.aerosil.com/aerosil/en/industries/personalcare/haircare/ www.aerosil.com/aerosil/en/industries/personalcare/cosmetic/
[4] Grobe A, Renn O and Jaeger A 2008 *Risk Governance of Nanotechnology Applications in Food and Cosmetics* (Geneva: International Risk Governance Council) www.irgc.org/IMG/pdf/IRGC_Report_FINAL_For_Web.pdf
[5] Bharali D J, Klejbor I, Stachowiak E K, Dutta P, Roy I, Kaur N, Bergey E J, Prasad P N and Stachowiak M K 2005 *Proc. Natl Acad. Sci. USA* A **102** 11539
[6] Bottini M *et al* 2007 *Int. J. Nanomed.* **2** 227
[7] Hirsch L R, Stafford R J, Bankson J A, Sershen S R, Rivera B, Price R E, Hazle J D, Halas N J and West J L 2003 *Proc. Natl Acad. Sci. USA* A **100** 13549
[8] Roy I, Ohulchanskyy T Y, Bharali D J, Pudavar H E, Mistretta R A, Kaur N and Prasad P N 2005 *Proc. Natl Acad. Sci. USA* A **102** 279
[9] Verraedt E, Pendela M, Adams E, Hoogmartens J and Martens J A 2010 *J. Control. Release* **142** 47
[10] Nabeshi H *et al* 2011 *Biomaterials* **32** 2713
[11] Yamashita K *et al* 2011 *Nature Nanotechnol.* **6** 321
[12] Nabeshi H *et al* 2011 *Part. Fibre Toxicol.* **8** 1
[13] Hardisty R M and Margolis J 1959 *Br. J. Haematol.* **5** 203
[14] Bloom A L 1962 *J. Clin. Pathol.* **15** 508
[15] Cochrane C G and Griffin J H 1982 *Adv. Immunol.* **33** 241
[16] Colman R W and Schmaier A H 1997 *Blood* **90** 3819
[17] Vogler E A, Graper J C, Harper G R, Sugg H W, Lander L M and Brittain W J 1995 *J. Biomed. Mater. Res.* **29** 1005
[18] Vogler E A, Graper J C, Sugg H W, Lander L M and Brittain W J 1995 *J. Biomed. Mater. Res.* **29** 1017
[19] Vogler E A, Nadeau J G and Graper J C 1998 *J. Biomed. Mater. Res.* **40** 92
[20] Zhuo R, Miller R, Bussard K M, Siedlecki C A and Vogler E A 2005 *Biomaterials* **26** 2965
[21] Borm P, Klaessig F C, Landry T D, Moudgil B, Pauluhn J, Thomas K, Trottier R and Wood S 2006 *Toxicol. Sci.* **90** 23
[22] Nel A, Xia T, Madler L and Li N 2006 *Science* **311** 622
[23] Xia T *et al* 2006 *Nano Lett.* **6** 179
[24] Rahman I A, Vejayakumaran P, Sipaut S C, Ismail J and Chee K C 2009 *Mater. Chem. Phys.* **114** 328
[25] Gorbet M B and Sefton M V 2004 *Biomaterials* **25** 5681
[26] Miller L L and Bale W F 1954 *J. Exp. Med.* **99** 125
[27] Miller L L, Bly C G, Watson M L and Bale W F 1951 *J. Exp. Med.* **94** 431
[28] Tennent G A, Brennan S O, Stangou A J, O'Grady J, Hawkins P N and Pepys M B 2007 *Blood* **109** 1971–4
[29] Gordon E M, Gallagher C A, Johnson T R, Blossey B K and Ilan J 1990 *J. Lab. Clin. Med.* **115** 463
[30] Tsuruta J, Yamamoto T and Kambara T 1986 *Adv. Exp. Med. Biol.* B **198** 63
[31] Nabeshi H *et al* 2011 *Nanosc. Res. Lett.* **6** 93

Arch Toxicol
DOI 10.1007/s00204-012-0823-5

INORGANIC COMPOUNDS

Suppression of nanosilica particle-induced inflammation by surface modification of the particles

Tomohiro Morishige · Yasuo Yoshioka · Hiroshi Inakura · Aya Tanabe · Shogo Narimatsu · Xinglei Yao · Youko Monobe · Takayoshi Imazawa · Shin-ichi Tsunoda · Yasuo Tsutsumi · Yohei Mukai · Naoki Okada · Shinsaku Nakagawa

Received: 17 August 2011 / Accepted: 27 February 2012

Abstract It has gradually become evident that nanomaterials, which are widely used in cosmetics, foods, and medicinal products, could induce substantial inflammation. However, the roles played by the physical characteristics of nanomaterials in inflammatory responses have not been elucidated. Here, we examined how particle size and surface modification influenced the inflammatory effects of nanosilica particles, and we investigated the mechanisms by which the particles induced inflammation. We compared the inflammatory effects of silica particles with diameters of 30–1,000 nm in vitro and in vivo. In macrophages in vitro, 30- and 70-nm nanosilica particles (nSP30 and nSP70) induced higher production of tumor necrosis factor-α (TNFα) than did larger particles. In addition, intraperitoneal injection of nSP30 and nSP70 induced stronger inflammatory responses involving cytokine production than did larger particles in mice. nSP70-induced TNFα production in macrophage depended on the production of reactive oxygen species and the activation of mitogen-activated protein kinases (MAPKs). Furthermore, nSP70-induced inflammatory responses were dramatically suppressed by surface modification of the particles with carboxyl groups in vitro and in vivo; the mechanism of the suppression involved reduction in MAPK activation. These results provide basic information that will be useful for the development of safe nanomaterials.

Keywords Inflammation · Macrophage · Nanoparticle · Silica · Surface modification

Abbreviations

BHA	Butylated hydroxyanisole
DPI	Diphenyleneiodonium chloride
ELISA	Enzyme-linked immunosorbent assay
ERK	Extracellular signal-regulated kinase
IL	Interleukin
JNK	C-jun N-terminal kinase
KC	Keratinocyte chemoattractant
MAPKs	Mitogen-activated protein kinases
MCP-1	Macrophage chemoattractant protein-1
PBS	Phosphate-buffered saline
PCLF	Peritoneal cavity lavage fluid
ROS	Reactive oxygen species
TEM	Transmission electron microscopy
TNFα	Tumor necrosis factor-α

T. Morishige · H. Inakura · A. Tanabe · S. Narimatsu · X. Yao · Y. Mukai · N. Okada · S. Nakagawa (✉)
Laboratory of Biotechnology and Therapeutics, Graduate School of Pharmaceutical Sciences, Osaka University, 1-6 Yamadaoka, Suita, Osaka 565-0871, Japan
e-mail: nakagawa@phs.osaka-u.ac.jp

Y. Yoshioka · S. Tsunoda · Y. Tsutsumi · S. Nakagawa
The Center for Advanced Medical Engineering and Informatics, Osaka University, 1-6 Yamadaoka, Suita, Osaka 565-0871, Japan

Y. Yoshioka · S. Tsunoda · Y. Tsutsumi
Laboratory of Biopharmaceutical Research, National Institute of Biomedical Innovation, Osaka 567-0085, Japan

X. Yao
Institute of Pharmaceutics, Zhejiang University, 388 Yuhangtang Road, Hangzhou 310058, China

Y. Monobe · T. Imazawa
Laboratory of Common Apparatus, Division of Biomedical Research, National Institute of Biomedical Innovation, Osaka 567-0085, Japan

Y. Tsutsumi
Laboratory of Toxicology and Safety Science, Graduate School of Pharmaceutical Sciences, Osaka University, Osaka 565-0871, Japan

Published online: 15 March 2012

Introduction

Many nanomaterials with innovative functions have been developed. For example, titanium dioxide nanoparticles, carbon nanotubes, and nanosilica particles have already been used commercially in electronics, medicine, cosmetics, and foods. Amorphous (noncrystalline) nanosilica particles with extraordinary properties can be synthesized by straightforward methods and are relatively inexpensive, and surface modification of the particles is easy to accomplish. In addition, they are usually considered to have low toxicity, in contrast to crystalline silica, which can cause silicosis and some forms of lung cancer (Huaux 2007; Mossman and Churg 1998). Therefore, nanosilica particles have been used for many applications, including cosmetics, foods, medical diagnosis, and drug delivery (Bharali et al. 2005; Bottini et al. 2007; Hirsch et al. 2003; Roy et al. 2005; Verraedt et al. 2009).

However, the increasing use of nanomaterials has raised public concern about their safety (Kagan et al. 2005; Nel et al. 2006). Carbon nanotubes have been reported to induce mesothelioma-like lesions in mice upon injection (Poland et al. 2008; Takagi et al. 2008), in a similar manner to crocidolite asbestos, and to suppress the immune system and damage DNA (Mitchell et al. 2009; Yamashita et al. 2010). Furthermore, nanosilica particles have been reported to induce oxidative stress, genotoxicity, and inflammation in vitro and in vivo (Chen et al. 2008; Liu and Sun 2010; Yang et al. 2010). Because inflammation has been implicated as the key factor in the development of chronic obstructive pulmonary disease, fibrosis, and carcinogenesis (Dostert et al. 2008; Mantovani et al. 2008), the need to investigate the inflammatory effects of nanosilica particles and ensure their safety is urgent.

Our group and others have recently reported that the characteristics of particles, including size and surface properties, are important factors in pathologic alterations and cellular responses (Albrecht et al. 2004; He et al. 2008; Morishige et al. 2010a, b; Waters et al. 2009; Yamashita et al. 2011). For example, we showed that administration of nanosilica particles into pregnant mice induces pregnancy complications, whereas microsilica particles have no effect (Yamashita et al. 2011). Furthermore, Decuzzi et al. (2010) demonstrated that the biodistribution of silica particles depends on particle size. However, only a few studies have assessed the roles of the physical characteristics of nanomaterials in relation to the inflammatory responses they induce. Therefore, the relationship between nanoparticle characteristics and biological effects, including inflammatory effects, and the precise mechanisms of these effects must be investigated. In addition, the results of such investigations should be used to develop a methodology for decreasing the adverse biological effects of nanomaterials.

In this study, we evaluated the correlation between inflammatory effects and the size and surface modification of silica particles. Furthermore, we investigated the mechanisms of the inflammatory responses induced by nanosilica particles.

Materials and methods

Materials and reagents

Unmodified amorphous silica particles with diameters of 30, 70, 300, or 1,000 nm (designated nSP30, nSP70, nSP300, and mSP1000, respectively) and nSP70 with surface carboxyl groups (nSP70-C) were purchased from Micromod Partikeltechnologie (Rostock/Warnemünde, Germany). Butylated hydroxyanisole (BHA) and diphenyleneiodonium chloride (DPI) were purchased from Sigma-Aldrich (St. Louis, MO). Rabbit polyclonal anti-phospho-p38 antibody (sc-17852-R) and mouse monoclonal anti-β-actin antibody (sc-47778; clone C4) were purchased from Santa Cruz Biotechnology (Santa Cruz, CA). Rabbit polyclonal anti-extracellular signal-regulated kinase (ERK)1/2 antibody (#9102), rabbit polyclonal anti-c-jun N-terminal kinase (JNK) antibody (#9252), rabbit monoclonal anti-phospho-JNK antibody (#4671; clone 98F2), and goat anti-rabbit peroxidase-conjugated antibody (#7074) were purchased from Cell Signaling Technology (Danvers, MA). Rabbit monoclonal anti-phospho-ERK1/2 antibody (MAB1018; clone269434) was obtained from R&D Systems (Minneapolis, MN). Rabbit polyclonal anti-p38 antibody (ab47437) was purchased from Abcam (Tokyo, Japan). Goat anti-mouse peroxidase-conjugated antibody was purchased from SouthernBiotech (Birmingham, AL). p38 inhibitor SB203580, ERK inhibitor U0126, and JNK inhibitor SP600125 were obtained from Merck (Darmstadt, Germany).

Cells and mice

RAW264.7 (mouse monocyte/macrophage cell line) cells were obtained from the American Type Culture Collection (Manassas, VA) and cultured at 37°C in Dulbecco's modified Eagle's medium (Wako Pure Chemical Industries, Osaka, Japan) supplemented with 10% fetal bovine serum and antibiotics. Female BALB/c mice were purchased from Nippon SLC (Shizuoka, Japan) and used at 8 weeks of age. All the animal experimental procedures were performed in accordance with Osaka University's guidelines for the welfare of animals.